Dean effect in particle sorting

Master's thesis, 15.7.2021

Author:

Julianna Heikkilä

Supervisors:

Andreas Johansson
Gianmario Scotti

JYVÄSKYLÄN YLIOPISTO
FYSIIKAN LAITOS

Abstract

Heikkilä, Julianna
Particle sorting with a device utilising Dean effect
Masters's thesis
Department of Physics, University of Jyväskylä, 2021, 51 pages.

A particle sorting device was made in this study with the particles being separated according to their size. This type of device can be utilised in applications requiring enrichment or concentration. The device designed is fabricated from PDMS and it has a 1.5-loop spiral geometry. The sorting is caused by hydrodynamic forces acting on the particles flowing in a microchannel. Dean effect, caused by curvature of the channel, enhances the separation. It leads to 31.5 µm sized particles to be sorted from 14.3 µm and 5.1 µm sized particles. With the plastic particles, the device demonstrated a separation efficiency of up to 94%. The results could be improved by additional components for the device or the set-up, and by modifying the image analysis script. Optimising the conditions further, the device could be applied to circulating tumour cell separation, or other biological and medical applications.

Keywords: Dean effect, microfluidics, particles, separation, sorting

Tiivistelmä

Heikkilä, Julianna
Partikkelien lajittelu Deanin efektiin pohjautuvalla laitteella
Maisterin tutkielma
Fysiikan laitos, Jyväskylän yliopisto, 2021, 51 sivua

Tässä tutkielma suunniteltiin ja valmistettiin partikkelien lajitteluun tarkoitettu laite. Kyseinen laite hyödyntää toiminnassaan hydrodynaamisia voimia ja Deanin efektiä. Partikkelit saadaan eroteltua niiden koon perusteella. Laitetta voidaan hyödyntää partikkelien konsentraation kasvattamiseen. Laite on puolentoistakierroksen mallinen spiraalikuvio ja se valmistetaan PDMS:stä. Tutkimuksessa lajiteltiin 31,5 µm, 14,3 µm ja 5,1 µm kokoluokan muovipartikkeleita. 94% isoimman kokoisista partikkeleista saatiin kerättyä. Tuloksia voitaisiin parantaa muokkaamalla mittausasetelmasta kattavampi tai kuvankäsittelystä tarkempi. Tulevaisuudessa laitetta voitaisiin hyödyntää syöpäsolujen erottamiseen verinäytteistä tai muihin biologisiin ja lääketieteellisiin sovelluskohteisiin.

Avainsanat: Deanin efekti, mikrofluidistiikka, partikkelit, lajittelu

Contents

1 Introduction

Transport of material or biological targets is one facet of the field called microfluidics. It is particularly attractive in regard to cells and bacteria which have been heavily studied for some time now. The reason being, microfluidics strikes a balance between enough energy required for biological targets and small enough dimensions for adequate control. Reagent and sample volumes are kept small, which is another benefit. Lab chips in various designs are classic examples of microfluidic devices. There, targets are transported through various sites, where different analysis functions can be performed.

In fact, many microfluidic applications are ultimately downscaled versions of existing approaches. However, fabrication of the device is not that straightforward, because of scaling laws. It means matter behaves differently in microscale than in bulk. Direct downscaling is not possible in many cases. On the flip side, many phenomena rising from microscale dimensions can be utilised in microfluidics.

Microfluidic devices offer portability, accessibility, and low cost. To study microorganisms, the option to manipulate, sort, separate, immobilize, and conduct other similar actions is desired. Using passive hydrodynamic forces in microfluidics has emerged as robust, simple, and versatile solution. Passive microfluidic devices are typically easy to fabricate and simple to operate. Fast liquid flows are usually quite obtainable as well. It means processing times are quick, and many samples can be analysed in a reasonable time. Forces arising from the conditions present in the microfluidic set-up govern the operation. For example, lift forces arising from the presence of a wall, or nearby particles. Another example is Dean drag force.

Size, deformability, and density are common characteristics of particles which are utilised in the operation of microfluidic devices. The first of which is typical in cases involving the Dean drag force. The Dean effect is caused by curvature in a microfluidic channel leading to a centrifugal like force. Vortices are formed perpendicular to the flow, which results in certain equilibrium positions for the particles. They vary across the channel width depending on their size. The curvature and geometry of the channel as well as viscosity, density and velocity of the fluid

affect the magnitude of the Dean force. Particle separation is a prime use for this technology as targets can be distinguished by their size alone.

When designing a microfluidic device intended for particle separation with Dean effect, channel dimensions have a massive impact on the separation efficiency. The height, width, and length of the channel all influence the possible equilibrium positions particles can have in the channel. In addition, suitable design can ease both the fabrication of the sample, and the use of the device. Most common designs are spiral, where controlling curvature is relatively easy. Inlet(s) and outlet(s) are simple to place, and the devices can be cascaded quite effortlessly. Such devices have been made by Warkiani et al. [1]. Other types of microfluidic designs are straight with islands, sinusoidal or square wave shaped, ones with many bifurcations, and those that combine all the previous elements. Devices from Mutt et al. [2] and Edd et al. [3] are examples of the island type.

Several methods for particle separation exist, ranging from antigen-antibody based to label-free, and from active "one particle at a time" -methods to continuous rapid devices. However, many of them have the issue of damaging particles, clogging channels, insufficient specificity, low purity, inducing cytotoxicity, or slow operation. With microfluidics, most of these issues can be tackled with an optimised design of the device. Some of the existing devices have already been commercialised and have seen success in applications such as cancer diagnostics, catalyst creation, and nanostructure functionalisation.

The aim of our research is to further improve spiral inertial microfluidic chip devices to obtain fast, continuous, reliable, and label-free particle sorting. Reducing the cost of fabrication and improving the efficiency of particle separation is done through simplifying the process. In the fabrication of the device, negative resist photolithography is used to create a silicon mould. A polymer mixture is then cast onto the mould creating the backbone of the device. Several chips are made from a single batch, each with a spiral pattern to facilitate particle separation using Dean effect. Polystyrene particles are used in the measurements to separate them based on their size. The device is intended to be a part of a larger chain of devices, which will provide a comprehensive sorting and analysis of particles. Potentially, it could be used in medical applications.

2 Microfluidics

In microfluidics, flows are constrained to small scales, typical dimensions are in the order of a few hundred micrometres. This applies to one dimension in the system, such as diameter of a pipe or width of a channel. Other dimension like length can be several meters long. Microfluidic systems commonly process volumes in tens to hundreds of millilitres at best. Microfluidics, in other words, is a study of flows and their behaviour in small volume systems. There is a potential for precise control of the microflows and the ability to manipulate them. Adequate control is necessary to handle and detect even the smallest possible particles present in a liquid. The flows can be in one or several phases, and the liquids can be simple or complex solutions. The phases can be liquid and gas, or liquid and droplets, for instance. [4–6]

Man-made systems are not all that microfluidics encompasses. Microsize systems can also be found in nature. Trees, plants, and fungi with their complex network of capillaries are an example of controlled circulation in nature's systems. Spider silk for spider webs is an example of transport and chemical reaction microfluidics. In spider's silk glands, silk proteins in gel-like form are pulled through a duct lined with cells and molecules doing processes such as ion exchange [7]. In humans, transport of cells through some membranes are done with capillary channels. An example of this is depicted in Figure 1, where blood cells are transported into the brain through capillaries. Most systems made by man pale in comparison to natural systems. However, microfluidics devices have become an important tool in biotechnology and are ever developing. [4–6]

One trending application for microfluidics is manipulation and transportation of cells. The ability to separate, immobilize, concentrate, sort and mix cells are useful functions for a myriad of biotechnological devices. Examples of such are rachets for cell separation [9], recirculating chambers for cell cultures [10], and intersections both for mixing and imaging [11]. Micro-and nanoparticles, macromolecules, and cells are all targets for microdevices. Often processing contains multiple steps from transport using microflows and droplets to manipulation of particles with magnetic, electric and optic methods. [5]

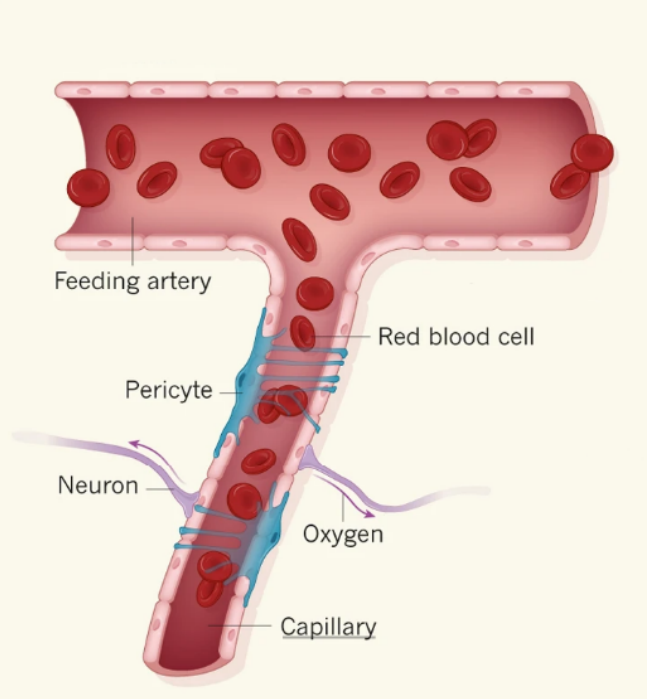

Figure 1. An example of a natural microfluidic system: capillary transporting red blood cells to brain from an artery. Image from Greif and Eichmann [8], edited for clarity.

2.1 Microscopic scales

Many properties of fluids and particles in microfluidics are due to microscale phenomena, which arise from the small dimensions in the systems. In micro- and nanoscale, surface areas are comparable to their volume. However, intermolecular distances are much smaller than the dimensions of the system. The latter means the identity of individual atoms can be disregarded, while the former means volume forces, like gravity, are unimportant in microfluidic systems. Instead, surfaces forces, such as frictional forces, dominate. Additionally, electrical, magnetic, surface tension forces can be predominant in microfluidic systems. [4]

Insect capable of walking on a liquid plane is an example of these beneficial scales. The gravitation force intends to immerse the insect into the liquid, while capillary forces from the water compensate it. Gravitational force affects object three-dimensionally, while surface tension is associated only with length. So, when small scales are considered, surface tension is far more dominant of a force when compared to gravity. Similarly, if cars are downsized to microscopic, a crash would occur when driving into a water droplet. [4]

Due to the dimensions of microscale devices, microfluidic systems are often considered to be in the transitional regime between small nanoscale molecular regime and large macroscale continuum regime. For example, boundary conditions are not the same for microsystems as they are for equivalent macrosystems. In most applications, microscopic size range is sufficient, and development in microfluidics is not focused on reducing the feature size of the device. Rather, it is about making more sophisticated and complex systems, ones that are integrable. [4]

The small scale causes changes in fluid behaviour, leading to various effects called breakdown phenomena. They occur when scaling down from bulk, and all the classic forces and laws no longer hold. It typically happens on the micro- and nanoscale. These phenomena can be utilised in microfluidic approaches as it leads to new effects or higher performance. For example, the dominance of surface tension over gravity is utilised in droplet microfluidics. [6, 12]

2.2 Laminar flow

A substance is considered a fluid when exhibiting continuous strain upon subjection to shear stress. In other words, substance has continuous deformation under pressure. They have no elastic stiffness, and thus cannot resist any stress. The shear stress, τ, to shear velocity is given by viscosity μ. When the gradient of flow velocity, v, is not linear to the dimension y, perpendicular to flow direction, the relation can be expressed as

$$\tau = \mu \frac{dv}{dy}.$$

Specifically, the viscosity in question is dynamic viscosity, not to be confused with kinematic viscosity. Kinematic viscosity, υ, relates dynamic viscosity to density, ρ. With higher viscosity, the fluid tends to be thicker. That is but one characteristic of fluids viscosity predicts. Viscosity is an important property of a fluid. [13]

A fluid flow is considered laminar when viscous forces are more dominant than inertial forces. This applies regardless of whether the flow is microscopic or macroscopic. Flow lines are at least locally parallel, and turbulence cannot develop. Laminar flow, and its counterpart turbulent flow, are shown in Figure 2. Despite no trubulence with laminar flow, recirculation can still be present. It does not equate turbulence. Most microflows tend to be laminar due to small dimensions in the system. Channel walls are in close proximity to each other which limits vortex development and randomness.

The laminar nature of microflows permit multiphase reactions, solvent exchange, filtering, and other tasks useful in microfluidic applications [5]

For laminar flows, the velocity profile is parabolic. Therefore, particles do not all experience the same velocity. For average velocity, it depends on the channel dimension and the flow rate. The average velocity can be calculated using the following formula

$$\overline{v} = \frac{s}{t} = \frac{V}{At} = \frac{Q}{A}, \tag{1}$$

where s is the travelled distance for the particle, t is the required time for travelling the distance, V is the volume the flow travels, A is the area of the channel cross-section and Q is the flow rate. [14]

When shear stress and shear rate relation is linear, a fluid is considered a Newtonian fluid. In other words, the liquid has constant viscosity. If viscosity does not remain constant, the fluid is non-Newtonian. For example, water is a Newtonian fluid, while blood is non-Newtonian. Blood has relatively high viscosity at low shear rate because it induces aggregation of blood cells. [13]

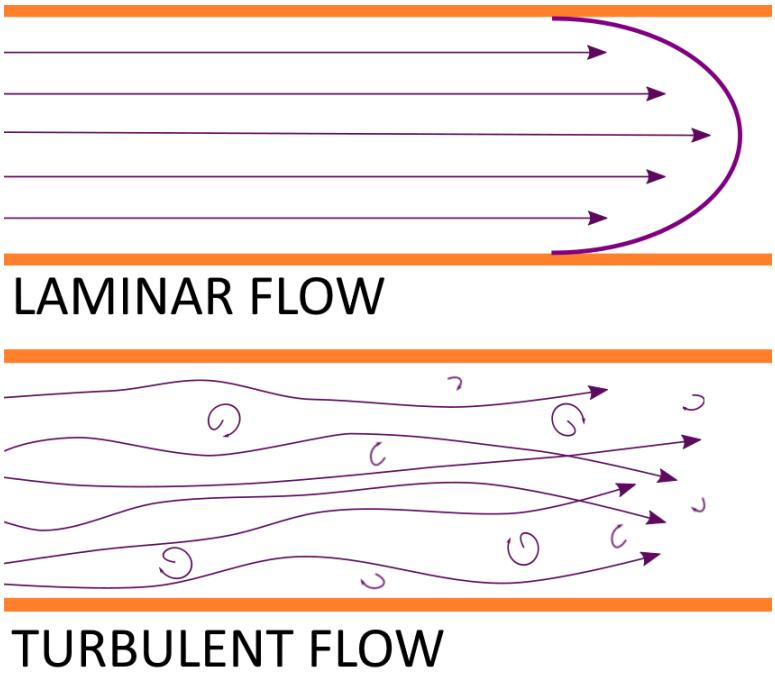

Figure 2. Illustration of laminar flow (top) and turbulent flow (bottom) in a microfluidic channel. Arrows represent velocity profile of the flow. The shape of laminar flow velocity is parabolic, while for turbulent it is irregular

2.2.1 Reynolds number

The ratio between convective (inertia) forces and viscous forces is called Reynolds number, which is defined as

$$Re = \frac{\overline{v}\rho L}{\mu}, \tag{2}$$

where μ is the dynamic viscosity, $\overline{v}$ is the average fluid velocity, ρ is density of the fluid, and L is the length of the microchannel in the system. [4, 5, 13, 15]

In other words, with Reynolds number, inertial effects of the flow are compared to viscous effects. In microfluidics, with low Re values being typical, microflows are heavily dominated by viscous effects. Reynolds number is a non-dimensional number and holds no unit. It is the most common non-dimensional number in microfluidics. It characterises the fluid flow in confined volumes. Importantly, it is a property of the flow, not the fluid.

Reynolds number also indicates whether flow is laminar, transitional, or turbulent. These correspond to values of up to 2000, between 2000 and 10 000, and above 10 000, respectively. In microfluidics, with a tendency for small Reynolds numbers, laminar flow is consequently ubiquitous. The small Reynolds number is a consequence of low velocities and small length scales. Commonly, Reynolds numbers in microfluidic flows are way below a thousand, often smaller than 1. In flows with low Reynolds numbers, turbulence and hydrodynamic instabilities are nearly non-existent. However, flows with medium ranged Reynolds number, e.g. 1-20, have properties that are useful for microfluidic applications. In a curved channel, one such effect is spiral streamlines caused by a centrifugal effect. [5, 13, 16]

As an example, Reynolds number is 0.2 for water flowing at 1 µl/min flow rate through a microchannel of 100 µm in diameter. The flow is undoubtedly laminar since the limit for turbulence is far greater than 0.2. Surface roughness, entrance regions, wall slip, dissipation and non-Newtonian fluids are an exception to turbulent conditions. In these cases, it is possible perturbations to exist in laminar flow even with low Reynolds numbers. [13]

Moreover, Reynolds number has been linked to the probability on the occurrence of recirculation. For it to happen, Reynolds number needs to be sufficiently large, and particularly the depth of the channel should be greater than the width. The smaller the ratio, the smaller the recirculation velocity. Unlike turbulence, recirculation is more exploited in microfluidics. They are a useful feature in mixing and homogenising

liquids, or in transport of targets to an area in the case of a reaction site. Trapping biological objects is another example. Obtaining recirculation passively is no easy feat, rather they are usually done with external fields. Small inertia, which flows with small Reynolds number have, as well as friction on the walls of the channel, particularly top and bottom, are the biggest reason for the emergence of recirculation. [5]

Maximum Reynolds number, at which laminar flow is sustainable, is called critical Reynolds number. Not only is critical Reynolds number larger for a curved channel than a straight channel, but it is larger for a more curved channel as well. Conversely, critical Reynolds number can be thought of as the Reynolds number at which laminar flow is sustainable through various coil curvature ratios. As curvature ratio consists of coil curvature diameter to channel inside diameter, laminar flow can be withstood up to Reynolds number 15 000 with a small curvature ratio of nine. [16]

2.2.2 Friction factor

In a channel, there is pressure loss along the length of it due to friction at the walls. Friction factor relates that pressure loss to the average velocity of fluid flow. Channels with circular cross-sections have a lower friction factor than channels with elliptical cross-section. In other words, the flow experiences less resistance in a circular channel. Channel wall's roughness and channel dimensions also impact friction factor. [4, 16]

Friction factor is expressed by Darcy-Weisbach equation $\Delta p/L$. When a fluid is incompressible and its flow is laminar, the exact solution is k/Re, where $48 \leq k \leq 96$. For a rectangular channel, $k \approx 76.8$. From the equation, it can be seen that the friction factor depends on the Reynolds number of the flow. Moreover, when channel size is reduced by a factor of 10, the fluid resistance increases by a factor of 10 000. [4, 13, 16, 17]

2.2.3 Slip condition

Ideally, the velocity of a liquid flow at a contact of a solid surface, like a channel wall, is zero. However, often friction or perturbation at the wall does not cause enough resistance to affect the flow velocity so greatly. When the mechanical energy of the fluid is greater, there is a tendency for slip. It means that there is less of a difference between the velocity of fluid on the surface and the velocity of fluid near the boundary. Same goes for any particles present in the fluid. Usually, slip velocity is in the order of a few m/s. [4]

It is possible for there to be no slip. This occurs when the velocity of the fluid near the boundary is the same as for the boundary itself. If the channel is stationary, it means that the flow velocity at the wall is zero. Both slip and no-slip conditions are depicted in Figure 3. Slip is only observed for polar liquids. However, it has been observed that for water, the no-slip condition is valid. A larger dipole moment of the liquid means and increase in slip. In the slip flow case, the hydrodynamic force is smaller than in the no-slip case.[4]

Surface properties of the solid affect slip velocity in the fluid the most. Firstly, geometric properties, like roughness. Roughness induces perturbation in the flow which dissipates the mechanical energy. Consequently, overall resistance of the flow is increased, and the tendency for slip decreases. Second, chemical properties, like hydrophobicity. Often, slip velocity arises from nanobubbles trapped in nanocavities at the surface. Localised defects increase the possibility of slip flow, for example dissolved gases or bubbles near a solid [4]

Slip can be apparent slip or true slip. The former occurs at fluid-fluid interface when a thin layer is bound to a solid surface. The latter occurs instead on the actual solid-liquid interface where liquid molecules truly slide on the solid surface. With true slip, viscous force between liquid molecules is stronger than between liquid and solid molecules. [4]

The slip flow phenomenon can be utilised in some practical applications. The presence of slip flow can be manipulated to be present and used to enhance mixing. It is beneficial to use slip flow to help in mixing applications as turbulence is often hard to generate in micro-and nanofluidics. Aside from mixing enhancement, slip flow can be used to reduce drag in the flow. Often, when flow velocities are far larger, slip velocity can be ignored. [4]

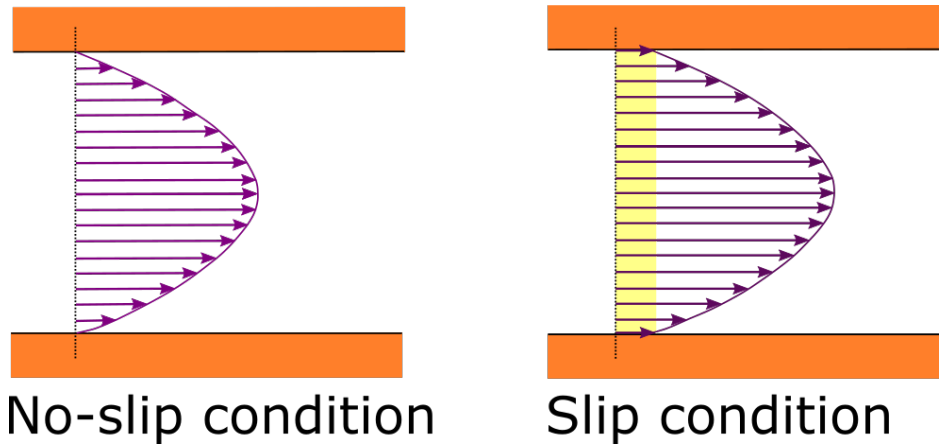

Figure 3. Potential slip velocity illustrated on a microchannel. Left, when flow has no slip. Right, when there is slip velocity.

2.3 Inertial microfluidics

Inertial microfluidics has recently risen as a term to represent faster microflows. Typically inertial forces are neglible as viscous forces dominate in microflows. However, with larger Reynolds numbers which inertial microfluidics encompass, that is not true. The rise of inertial forces lead to some valuable properties for the systems. Among those are Dean effect and lift forces, which often serve a function in cell separating, focusing, transferring, ranking, mixing, storing, manipulating, immobilising, and trapping. Inertial microfluidics is specifically suitable for cell and bacteria because of their size. They require sufficient energy available in faster flows, but too high velocity would compromise control. Though inertial microfluidics often lack specificity, the micro-and nanoscales combined with fast flow rates offer high throughputs with easy operation. [18, 19]

Hydrodynamic forces are at the forefront of inertial microfluidics. Various microdevices take advantage of these forces, to focus particles on equilibrium positions in the flow. Utilising these forces in the devices typically allows for simple operation and device structure. The forces used are typically inherent due to the dimension and geometry of the devices and the faster flows used. Thus, external fields are often not required in the operation. In addition, inertial microfluidic devices often have good performance in manipulating targets. Due to the fact, many of the most important applications are in biomolecule pre-treatments such as focusing and separation. The existing applications are considerably developed and utilised in so many aspects of life sciences and biomedicine. [18]

Inertial microfluidics has many beneficial aspects to it. The operation is typically simple, in many cases only adjusting flow velocity will realize the objective. Microfabrication is often straightforward, as the structures are quite plain. Swift yet yielding experiments are practically a given for functional inertial microfluidic devices. Best of all, nearly all of the devices have zero cytotoxicity and have no effect on the biomolecule or cell vitality. It is a highly desirable feature in biomedical devices. It provides new effects not possible through conventional methods. [18]

2.4 Microfluidic applications

Thanks to the many advantages of microfluidics, it can be applied to several purposes. DNA focusing i.e., stretching it for imaging, detection of exosomes, droplet development, packaging of single cells, manipulation of pathogenic bacteria, and the acquisition of circulating tumour cells (CTCs) among other things. Transport of biological materials is typically considered the main purpose of microfluidics. Detecting and controlling chemical reactions is an added feature in many systems. Moreover, microfluidics is essential in pre-treatment of biomolecules. Techniques like mixing, enrichment, separation, focusing and trapping allow for individual processing and optimal conditions in further processing or analysis. [4]

These pre-treatment methods are developed extensively. As an example, focusing is an important part of pre-processing for on-chip flow cytometers. Separation, on the other hand, is utilised in many applications where it required to distinguish biomolecules. Separation is often done based on inherent properties such as size, biological immunity, dielectric, optical, or mechanical properties. They are commonly used with tumour cells, exosomes, bacteria, DNA, droplets. Non-inherent properties such as labels can also be used. [18]

Other applications include lab on a chip technologies and microarrays. These include DNA chips, for instance, which allow gene expression or transcription. Micrototal analysis systems also fall into the same category. Chemical and biological essays, compact heat exchangers, and electro-osmotic pumps are additional examples of technologies which utilise microfluidics in their operation. Smaller components like sensors, reactors, actuator and microreactors are as well. Some fuel cells and inkjets also carry technology of the microfluidic sort. [4, 6]

For inertial microfluidics, cell separation is perhaps the most widespread application. Differentiation and studying of single cells are possible and contaminant removal is straightforward. Cell separation has been used to separate cancer and tumour cells, bacteria, and exosomes from blood. This allows for bacteria to be enriched without cultures, for instance. Inertial microfluidic cell separation is fast, simple, and inexpensive, which is the opposite for traditional methods such as centrifuges and filters. The former is slow, laborious and error prone while the latter is easily clogged and potentially harmful for cells. [20]

In inertial microfluidics, devices can also be used for focusing. That allows for single cell imaging and analysis. Bubble and droplet manipulation is also an application of inertial microfluidics. They can be generated and then used for example to encapsulate cells in. While inertial microfluidics often lack in specificity, it can also be utilised in real-time particle detection. Applications have been made in bioaerosol tracking, for instance. On top of all that, inertial microfluidics is well suited for studying particle migration dynamics. [20]

Some microfluidic concepts or designs have made their way into consumer products as well. Sport shoes which contain automatic cushioning control, toys which possess smart features, water level controls in washing machines, and tire pressure gauges are examples of such products. Some devices have found multiple suitable applications, like disposable blood pressure transducers and micro heat exchangers. The former is used in respirators, kidney dialysis equipment, lung capacity meters, and various medical process monitors, while the latter is used in residential, commercial, and electronics cooling, manufacturing as well as automobiles. [4, 6]

2.5 Pros and cons of microfluidic approach

The small scales offer multiple advantages which are heavily utilised in microfluidic applications. Power consumption is typically small, yet the devices offer high throughput. They have the ability to detect and manipulate small volumes, which offers low consumption of reagents and less waste. Process parameters in many applications are straightforward to control. Also, many of the devices are easy and inexpensive to make, and process automation is often quite simple. Microfluidic devices can be portable, user friendly, i.e., easy to operate, and even potentially remotely operatable. [4]

Parallelisation is another feature which is often straightforward to implement. It leads to faster, highly repeatable experiments with superior performance. For example, microplates can have wells from several hundreds to thousands, enabling multiple parallel processes in one device. Microfluidic devices can also contain several components with different functionalities. The construction of these integrated chips brings versatility to microfluidic devices. [4]

One area microfluidics lacks in, though, is particle motion analysis. Many effects induced in microflows are difficult observe both in traditional microfluidics and much more so in inertial microfluidics, as the flows are faster. Another of the few downsides in microfluidics is the limited physical understanding behind the phenomena utilised in the devices. With continuous research that is trending, that has a high change of getting negated. [4]

2.6 Hydrodynamic forces

All along a channel there is a redistribution of energy in the flow. Inertia and gravity make for some of this energy loss, but most of it is due to pressure pressure. Pressure has the dimension of energy per unit volume. The gradients in pressure are one of the main causes for hydrodynamic forces. The forces are induced to even the pressure differences. In microfluidics, the hydrodynamic forces can be used to manipulate particles. More specifically, to control their equilibrium positions in the flow. These forces include non-linear forces, such as axial drag and lateral forces in various forms. [5, 18]

Aside from drag and lift forces, there are other forces which may need to be considered. While rigid spheres like plastic beads often behave quite ideally, biological samples like cells and bacteria are deformable. The deformation will induce an extra force affecting the migration. It is born at the interface of the deformable objects from stress, and velocities of themselves and the surrounding fluid. Additionally, the deformation will affect lateral migration. Any difference in density between the particle and that of the flow will affect the equilibrium positions of the particles as well. When densities are near identical, this inertial centrifugal force is ignorable. [18]

2.6.1 Drag force

As a particle flows in a fluid, it is subjected to a viscous drag force. It arises from a shear effect on the contact surface of the particle. An expression for the force is

$$F_{drag} = S \cdot f_d = 2\pi a \frac{f_d}{4}.$$

Here, S is the cross-section area of the particle, a its diameter, and f_d its drag coefficient. The drag coefficient depends on the relative velocity of fluid to particle, and the Reynolds number. [20]

Not only will drag force cause the particles to move along the main flow direction but they tend to have equal or nearly equal velocity as the liquid flow because of it. Since the particles have mass and volume, they do move slightly slower than the surrounding liquid. Drag force affects all particles in a liquid flow. They need to be relatively rigid particles to experiences a drag force in a flow, and the flow rates need to be moderate or fast. [5, 18]

2.6.2 Shear gradient induced lift force

In addition to drag force, lift forces are also present in the flow. They are hydrodynamic forces, which particles within a flow will experience. Based on their size, the particles migrate to equilibrium positions in the flow. The type and magnitude of lift forces depend on the particles distance to the wall of the channel. In microfluidics, lift forces are used to achieve purification, enrichment, focusing and separation of particles. [5, 18]

The main components of lift force are shear gradient lift force and wall induced lift force. The first results from the parabolic velocity profile of laminar flow. The flow is fastest in the centre of a channel, and slower towards the wall. Based on the particle's size, it experiences this gradience in velocity. The velocity of the particle is relatively larger on the side of the wall than on the side of the channel centre. [5, 18]

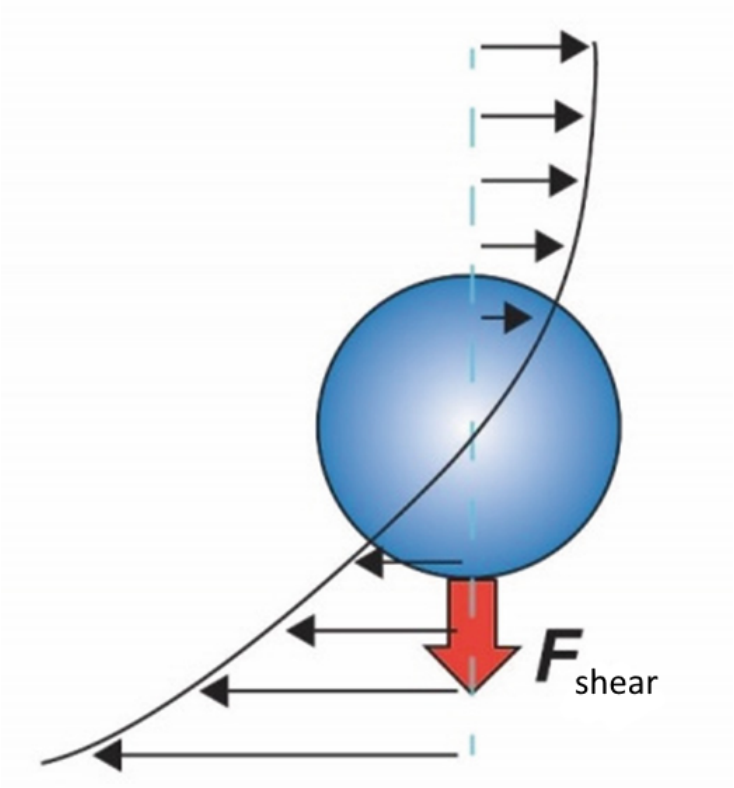

Figure 4. Shear induced lift force. Arrows represent relative velocity of the flow. Image from Ning et al. [21], edited for clarity.

The difference in pressure causes the particles to be pushed towards the wall. In other words, the shear gradient lift force is to the direction of the wall. The lift force depends on the carrier fluid density and velocity, the geometry of the channel, and the size of the particle. The shear gradient lift force is proportional in the following way:

$$F_{shear} \propto 2\rho U^2 a^3 / H.$$

Here, ρ is the density of the fluid, U is the velocity of the fluid, a is the diameter of the particle, and H is the hydraulic diameter. Particle under the influence of shear induced lift force is depicted in Figure 4. The shear gradient lift force is proportional to the square of the particle Reynolds number. For lift force to be effective on the particles in the flow, the Reynolds number must be great enough.In addition to lateral migration, the pressure difference from flow velocity profile causes spin on the particle. This is connected to vorticity present in the fluid. [5, 20]

2.6.3 Wall-induced lift force

The second component of lift force is associated with object's viscinity to a solid surface. Because particles rotate in a fluid flow, a symmetric wake forms around them. The wake can be affected due to proximity to a channel wall, should the particles migrate close enough. A force is induced to drive the particles further from the wall, to the direction of the centre. Vicinity of a wall causes relative velocity of the particle to be reduced on the side of the wall. This means that pressure on that side is greater than on the side of the centre. A lift force is induced in the direction away from the wall. The wall induced lift force's proportionality is expressed as

$$F_{wall} \propto \rho U^2 a^6 / H^4.$$

Here, ρ is the density of the fluid, U is the velocity of the fluid, a is the diameter of the particle, and H is the hydraulic diameter. Particle under the influence of wall induced lift force is depicted in Figure 5. [20]

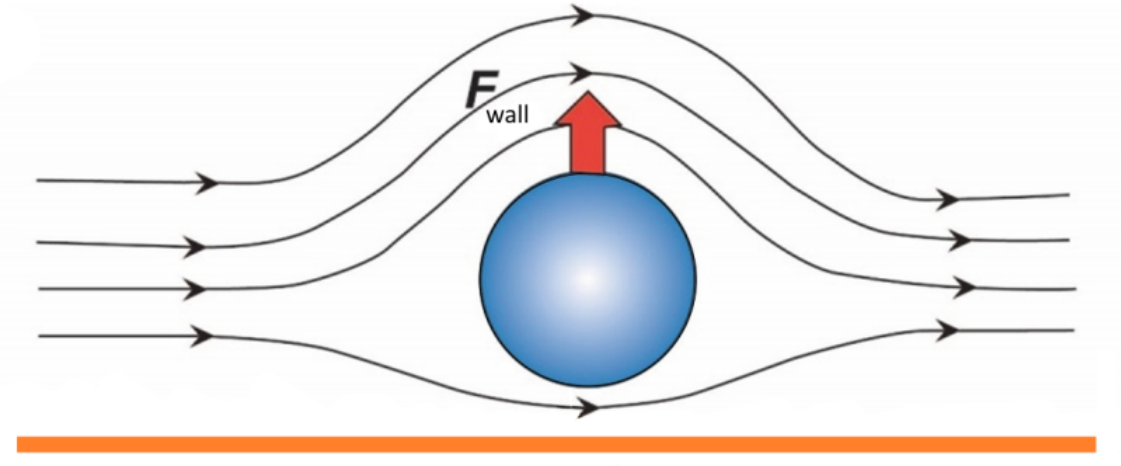

Figure 5. Wall induced lift force illustrated. Image from Ning et al. [21], edited for clarity.

Wall induced lift force is also sometimes called wake effect lift force. Both wall induced lift force and shear gradient induced lift force are proportional to the square of the particle Reynolds number. The particles must have a relatively high enough velocity for the lift forces to have a noticeable effect. As such, they are more utilised in inertial microfluidics. A Reynolds number larger than 1 for the flow is approximately sufficient for lift forces to be induced. Also, particle diameter needs to be sufficient for the particle to experience gradience laterally. [5]

The lift forces do not remain fixed, rather they vary along the microchannel length. If a particle migrates closer to the centre of the channel, shear gradient induced lift force becomes dominant, and pushes the particle away. Similarly, if a particle migrates closer to the wall, wall induced lift force dominates. In an equilibrium position for a particle, the lift forces are equal. Rigid particles typically are focused to a certain distance from the wall as a result of the two lift forces. [5, 18]

The migration of particles due to lift forces is lateral, perpendicular to the main direction of the flow. Though particles also experience gravity and buoyancy, they have negligible influence on the lateral location of the particles on the flow. They only affect the vertical position of the particles. Other forces exist too, but they are weak compared to lift forces, and thus often are disregarded. [18]

2.7 Dean effect

In a curved channel, a fluid has a higher velocity in the centre than near the wall regions. Because of inertia, particles in the curved channel tend to flow from the centre to the outer wall side. This leads to radial pressure gradient imbalance. A recirculation forms to balance the difference. Also, in closed channels, the mass conservation realises another pressure imbalance. The fluid from the outer wall recirculates inward. Two counterclockwise vortices are induced, which are called the Dean flow. The Dean vortices are towards the centre of the channel at the wall and away from it in the centre. [5, 15, 18]

Dean effect takes places in curved microchannels. The rotational effect requires sufficient inertia and pronounced curvature. The Dean effect happens in the plane of the cross-section, perpendicular to the main direction of the flow. The recirculation is induced to account for the relative pressure drop caused by curvature. Consequently, Dean effect stabilises the laminar flow and as a result, the critical Reynolds number is high. Turbulent flow starts at higher velocities for curved pipes than for straight

pipes. Capillaries can be operated to Reynolds number 15 000 before the flow cannot be considered laminar. [15]

In a straight channel, resistance is proportional to the flow velocity down to a minimum value. For curved channel, that value is smaller, because of the Dean flow. The vortices increases resistance at small flow velocities, keeping the flow steady. A critical value of velocity exists for a curved channel, where the Dean effect cannot keep the flow laminar. The critical value is so much greater for a curved channel than for a straight channel. A fluctuation, which is not diffusive in nature, is not likely to cause any increase in resistance of the flow. However, when there is diffusion of momentum, like in the Dean vortices, the resistance rises rapidly. [15]

In total, three forces are exerted on particles flowing in a curved channel: Hydrodynamic drag, lift forces and the Dean effect. The first transports the particles from an inlet to an outlet. The second force drives cells to certain equilibrium positions. The third, Dean vortices, reduce the equilibrium positions to one. The single position depends on the size of the particle. For smaller particles, it is near the outer wall. For larger, on the inner wall. Figure 6 shows the particles which have experienced lateral migration in a curved rectangular channel. [5, 18]

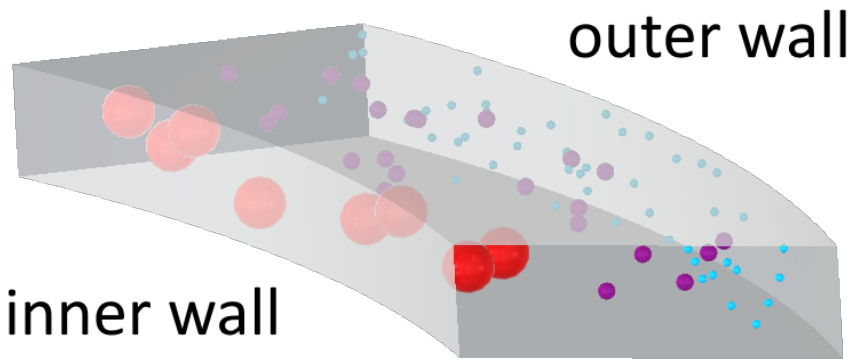

Figure 6. Lateral migration on a curved channel. Equilibrium positions tend close to the inner wall of the channel for the largest sized particle. In the image, red particles are the largest, purple particles the second largest and blue particles the smallest.

2.7.1 Dean number

A non-dimensional Dean number, De, characterises the flow in curved channels. It predicts the possibility of recirculation, for instance. It can be expressed as

$$De = Re\sqrt{\frac{D_H}{2R_c}}, \tag{3}$$

where R_c is the curvature radius of the curved channel, Re is the Reynolds number, and D_H is the channel's hydraulic diameter. The Dean number needs to be sufficiently large for the pair of vortices to form. A minimum of 0.1-1.0 realises the rotational effect. [5, 18]

Hydraulic diameter present in the equation is defined as $D_H = 4\frac{S}{p}$, where S is the cross-section of the channel and p is the wetted perimeter. The geometry and dimensions of the channel are what affect the hydraulic diameter. For a circular channel, D_H is the simplest, the same as its diameter. For a rectangular channel, it is $D_H = \frac{2ab}{a+b}$. [5]

The Dean number increases with increasing Reynolds number. Consequently, at higher flow velocities, the Dean number of the flow also changes. Additionally, it can also describe the shape of the Dean flow. Specifically, the location of the centre of the vortices. When Dean number is higher, the centre is closer to outer wall. In Figure 7, the vortices are visualized by a colour plot and velocity vectors. [18]

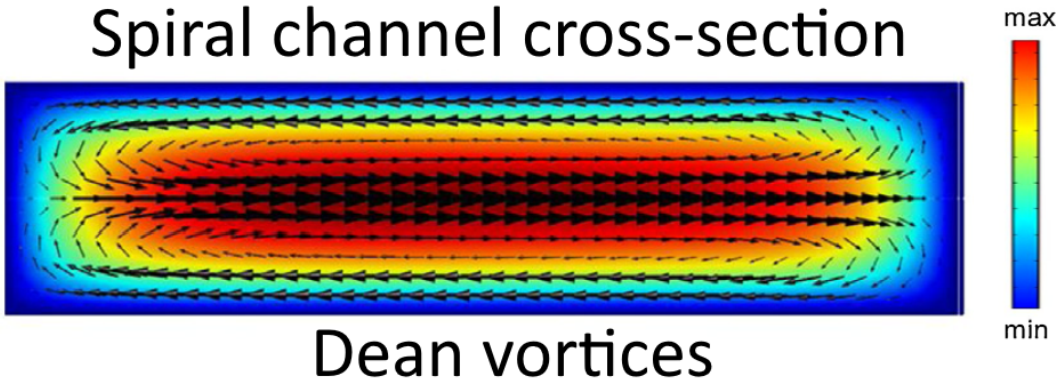

Figure 7. Dean vortices visualized with finite element analysis. Colour plot is the relative velocity field while arrows show secondary flow direction. Image from Asghari et al. [22], edited for clarity

The Dean force occurring on the particles induced from the vortices is proportional like

$$F_D \propto \ \rho v^2 a D_H^2 R_c^{-1},$$

where ρ is the density of the fluid, v is the velocity of the fluid, a is the diameter of the particle, R_c is the curvature radius and D_H is the hydraulic diameter. The magnitude of the force depends on the intensity of the flow velocity field. Similarly, the direction of the force depends on the direction of the flow velocity field at the cross-section. The particles will have equilibrium positions from the combined effects of inertial lift forces and Dean drag force. [18, 20]

Not only do the two counter-rotating vortices form from pressure gradients in curved channels, but at high flow velocities, secondary Dean vortices can form in the flow. They are formed due to increase in Dean number which leads to additional pressure gradient regions near the inner wall of the curved channel. They recirculate the fluid at the outer wall and enhance the particle sorting effect of Dean flow. In addition to flow velocity, the dimensions of the channel and radius of curvature influence the strength of the secondary Dean vortices as well. Decreasing curvature in relation to aspect ratio, will increase both Dean number and secondary Dean vortices formation probability. [18]

2.7.2 Dean effect in particle sorting

As Dean flow can influence the equilibrium positions of particles in the flow, it can be used in particle sorting. The particles are separated to different outlets in a microfluidic device based on their properties. Using Dean effect in spiral microfluidic channels offers high efficiency and high throughput. Sorting efficiency is often defined as the number of particles recovered from the total amount. For some implementations, a higher recovery rate is desirable, while for some higher purity is. The Dean flow accelerates lateral migration compared to just lift forces. It speeds up the focusing as particles reach their equilibrium positions faster. This needs to be taken into to account when designing the length of the curved channel. [5, 18]

When flow rates are high, particles tend to follow streamlines which pass by their centroid. Moreover, it has been observed experimentally that particles at a bifurcation tend to leave for the direction with a higher flow rate, with only very few flowing to the lower flow rate side. The reasoning behind it is the relative velocity

difference leading to higher pressure-gradient, drawing them towards the higher flow rate. Additionally, the flow rate difference is highly likely to cause torque on the particles. One factor causing the velocity difference at the bifurcation is unequal hydrodynamic resistance between the channels. With higher resistance, the flow rate is likely to be smaller. [5]

With the Dean effect, continuous separation of the particles is possible. An example of particle sorting with a two-outlet microchannel is shown in Figure 8. Many applications have turned up, which use Dean effect in sorting. This concept, for example, has been used by Bhagat, Kuntaegowdanahalli and Papautsky to separate neural cells in an Archimedean spiral device [23]. For blood cells, there have been many experiments, including by Wu, Guan, Hou, Bhagat and Han on leukocyte separation [24] as well as by Warkiani et al. on circulating tumour cell separation [1]. While Dean effect is popular in sorting applications, it can be used in mixing as well. [18]

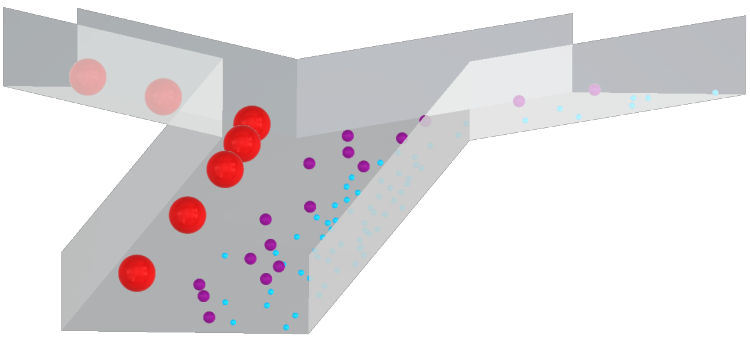

Figure 8. Illustration of particle sorting. Largest sized particles are flowing to inner wall outlet while smaller particles flow to outer wall outlet. It is a result of hydrodynamic forces in the liquid.

3 Measurements

The device designed and used for particle sorting in this study is a PDMS-glass chip. The geometry of the device is shown in Figure 9. It is a 1.5-loop spiral design. The fabrication of the chips consists of two parts. First, a SU-8 mould is made. Second, PDMS mixture is cast on the mould, cured and cut. With the individual PDMS chips, particle sorting measurements are done. Spherotech Inc. SPHERO™ crosslinked polystyrene particles are used in three different size ranges: 5.0 µm-5.9 µm, 13.0 µm-17.9 µm, and 25.0 µm-37.0 µm. Polystyrene particles with fluorescent properties were also used, in the same size ranges. The intention is to separate all of the largest sized particles from the others. This is because the device is intended to be used in a biological application, where circulating tumour cells (CTCs) could be separated from other types of cells in blood. The particle sizes chosen represent the actual cells: circulating tumour cells correspond with the largest size, white blood cells with medium size and red blood cells with smallest size.

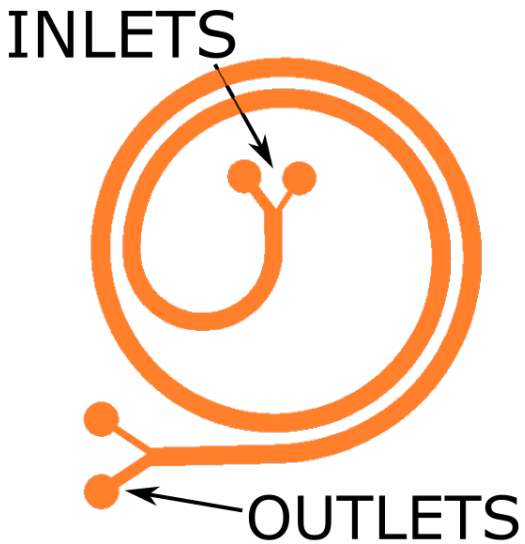

Figure 9. 2D model of device design. The geometry used is spiral, with two inlets and two outlets. The loops are circular. The device has 1.5 loops. Channel width is 500 µm and height is 170 µm

3.1 SU-8 mould

The mould used for casting the chips uses a silicon wafer as a base. A 4" wafer is used. It is cleaned with ethanol, IPA and compressed air. The wafer is HF treated to promote SU-8 adhesion. The treatment is a ten second bath in 10% HF solution. Before adding SU-8, the wafer is rinsed with DI water and dehydrated. Under 5ml of Gersteltec SU-8 photoresist (15-200 µm) is poured on the wafer. This is enough to cover it evenly, but bead on the SU-8 layer is minimised. The resist is spinned with a maximum speed of 575 rpm. This is followed by a pre-exposure bake. It consists of a planarization at 25 °C, and incubations at 65 °C and 95 °C.

The substrate is exposed to UV with a photomask containing the spiral design. It is the reverse image of the intended polarity for the PDMS chips. It allows the UV light through only at the spiral areas. Exposure is done using a mask aligner with a mercury lamp. The mask is aligned with the substrate and clamped to leave no gap. Exposure time is 230 seconds. After the exposure, SU-8 is post-exposure baked. This bake contains just 65 °C and 95 °C incubations, at shorter times than with the pre-exposure bake. Once the post-exposure bake is complete, the substrate can be developed. PGMEA (propylene glycol methyl ether acetate) is used as a developing agent for roughly ten minutes to remove unexposed SU-8. Light stirring is applied to enhance dissolving. Following the development, the wafer is cleaned resulting in the desired mould. The finished mould is shown in Figure 10.

Figure 10. Mould used for PDMS chips. It is made with negative photoresist SU-8 on a silicon wafer. It features the spiral design of the channels, in reverse.

3.2 PDMS chips

Before casting PDMS mixture on the mould, a fluoropolymer deposition with RIE or silanization treatment in a vacuum desiccator is done. It creates a thin film, which prevents PDMS from sticking to the mould.

Using SYLGARD 184 silicone elastomer kit, PDMS is prepared. A 10:1 ratio of base to curing agent (or 12.5:1 for a stickier finish) is used to form the mixture. For one batch of four PDMS chips, 1.8 and 18 g are weighed into a cup and mixed well. Before casting, air bubbles mainly resulting from stirring are removed. Vacuum desiccator is used for this purpose, with bubbles bursting due to low pressure. Once the PDMS mixture is uniform and bubble-free, it is poured onto the SU-8 mould. To ensure the mould stays put, it is taped onto a glass plate with a plastic rim or a petri dish.

Once any bubbles that have presented themselves during pouring have been delt with, the PDMS on the mould can be cured. 95 °C temperature is used with a baking time of an hour. Then, the resulting flexible PDMS disc can be peeled off from the mould. Each disc holds four individual strips with spirals, which form the channels. The strips are cut apart, and holes are punched through pads in the spiral design to form inlets and outlets.

To make devices from the PDMS strips, they are merged together with glass slides. Both PDMS strips and glass slides are treated with oxygen plasma to increase adhesion. Before treatment, both glass and PDMS strips are cleaned from dust and other contaminations. The glass slides are treated for longer and with higher power than the PDMS strips. Once both are treated, they are merged together. To enhance the adhesion, they are heated at 85 °C for an hour with a small weight on top. The fabricated PDMS chips are shown in Figure 11. The dimensions of the channels in the chips are 500 µm in width and 170 µm in height.

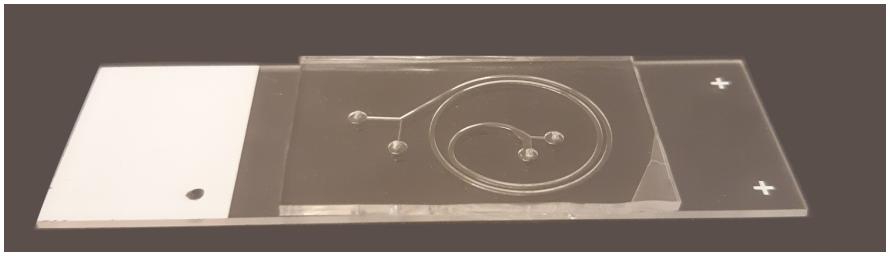

Figure 11. Image of the fabricated PDMS chip featuring the spiral design

3.3 Measurement set-up

To use the chips in an experiment, they are encased to allow tube connections. This jig can be seen in Figure 12 B). The case consists of a plastic top and bottom, with screws keeping them together. The top has metallic inlet and outlet pipes glued to it. The chips are inserted between the top and bottom, so that the metallic tubes align with inlet and outlet holes in the chips. Once the chips are secure in the case, tubes are added to provide passage for liquid flowing from syringe pumps to the channels in the chip.

The set-up includes two syringe pumps, one for sheath liquid and one for sample. They are from KD Scientific Inc. The sample syringe is connected to the smaller inlet in the chip and the sheath syringe to the larger inlet. The measurement set-up and equipment is shown in Figure 12 A). The sheath liquid consists of NaCl (5%) and DI water buffer solution, and the sample liquid consists of a mix of polystyrene particle solutions and the buffer solution. The polystyrene particles from the sample liquid experience combined flow rate from both syringe pumps in the channel of the chips. Flow rates used in the measurements ranged from 750 µl/min to 800 µl/min for the sheath pump. For the sample pump, flow rate was kept at a constant 100 µl/min.

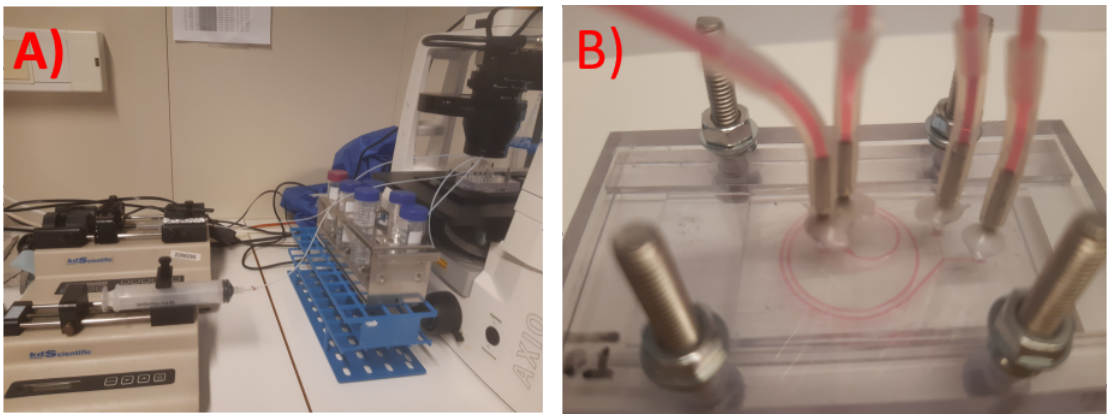

Figure 12. Image of measurement set-up. A) Sample and sheath (front) syringe pumps on the left, chip and case on the microscope on the right. Connecting teflon tubes from the pumps to the chip and from the chip to falcon tubes where elute is collected. B) A close-up of the chip in the case. Dyed water is used to show channels and connecting tubes better.

To analyse Dean effect in the flow, the chip is placed on an inverted microscope. Bright-field settings are used to see the standard particles, while fluorescent settings with a filter is used for the fluorescent variety. To capture the flow of the particles, a high-speed camera is mounted on the microscope. With it, the fast-moving particles can be imaged at the outlet.

3.4 Image analysis

By taking a stack of images, particles sizes and separation can be recorded. When analysing the images collected from the outlets, the sorting effectiveness of the design can be determined. Similarly, optimising flow rate for a sample is done. The image analysis is done with ImageJ software. The number of images a stack has depends on buffering time, full stack is 2863 images. All images are treated individually. The processing has three key steps: *background subtraction* (and *filtering*), *thresholding*, and *particle analysis*. In addition to these, *watershed* and *fill holes* methods are used to improve particle recognition. Some of the effects of methods on the image in the analysis process are shown in Figure 13.

Background subtraction minimises colour gradience in the background. With the set-up used in the work, the illumination on the outlet area is uneven. This means that areas of the images are lighter closer to the light source. Glue holding the metal tubes in the case creates shadow. For thresholding, where a good and constant contrast between target and background is key, subtracting background is essential. *Thresholding* sets a colour value limits for a greyscale image.

With a black and white image, binary operations can be used. Such is the case for *fill holes*, *watershed* and *analyse particles*. *Watershed* is used to distinguish cluttered objects in an image. The principle of operation is drawing separating lines on the areas where local minima (particles) start merging. It works best for two particle clusters or for particles touching each other lightly. *Analyse particles* distinguishes any black areas based on size and circularity. The values used in the methods are optimised by hand on a test image before processing a stack. Filters are optional but they can enhance both contrast and circularity of the particles.

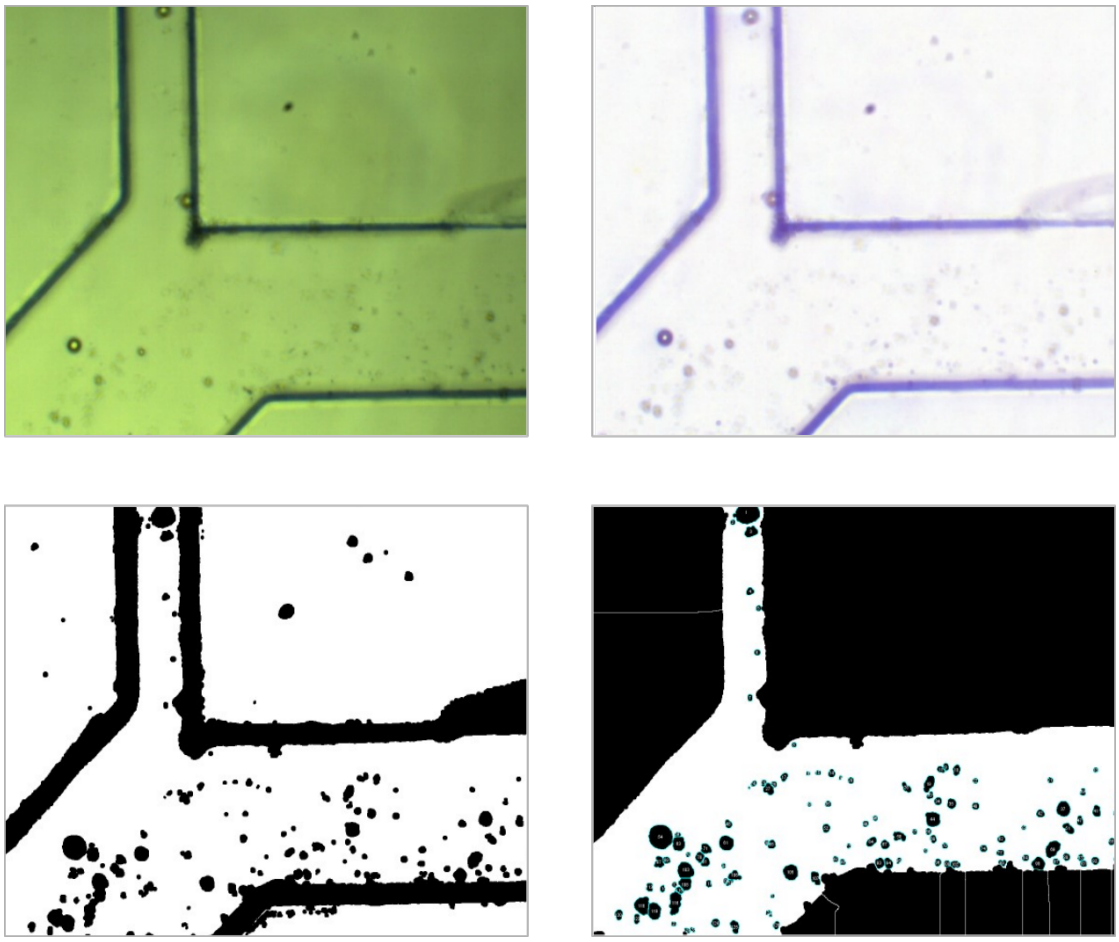

Figure 13. Progress in image analysis. Top left: original image obtained with high-speed camera. Top right: background is subtracted. Bottom left: Image is transformed to 8-bit and threshold is added. Bottom right: flood fill, filters, watershed and analyse particles is used

For counting of the particles, recorded area of the particle, starting x and y coordinates for the particle on the ImageJ's image coordinate system, and particle number assigned by the *analyse particles* method in ImageJ are used. Duplicates are removed using all of the data as parameters. This removes any stationary particles or contaminations mistaken as particles. Then, the particles are added together by their area and by the outlet they migrated to. For the former, lower and upper limits corresponding to each size range of particles is searched manually from the images and the recorded areas. For the latter, ImageJ's image coordinate system is used in conjunction with x and y start coordinates pf the particles to establish the correct outlet. In Figure 14, the parameters for particle addition are shown visualised on the outlet region.

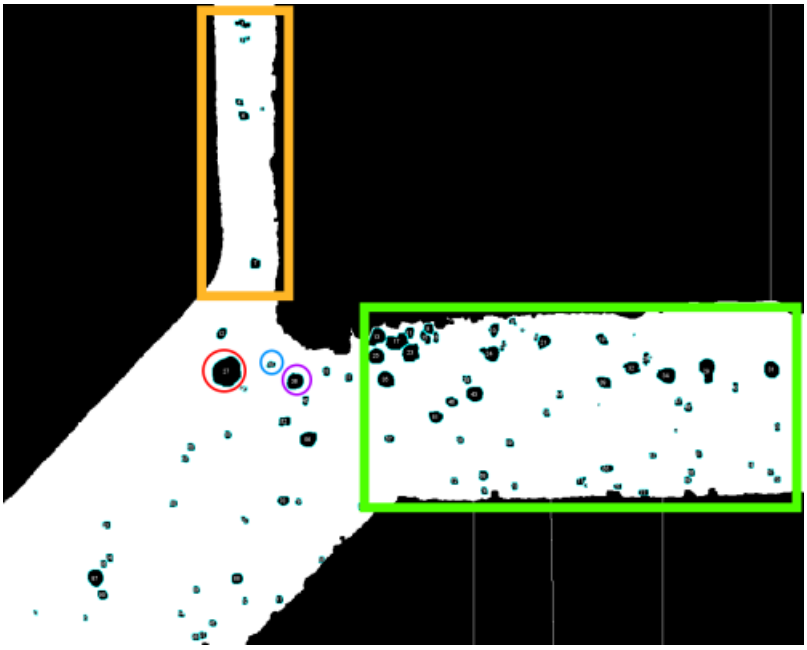

Figure 14. Particle counting parameters illustrated on top of an image obtained from image analysis. With large squares areas, from which particles are counted from, are illustrated. The orange square gives the limits for x start and y start coordinates the particles can have to be counted towards the inner wall outlet. The green square is the equivalent for outer wall outlet. With circles, the size examples for particle counting are shown. Particle circled with red has an area counted towards largest sized particles. Similarly, particle circled with purple is an example of medium sized particle area, and particle circled blue of the smallest sized area.

4 Results

A spiral Dean effect device was fabricated to act as a particle sorter. For studying whether the device was capable of any sorting, fluorescent particles were used see lateral migration in the channel. In Figure 15, the outlet region of the chip is shown, with fluorescent particles flowing in the channel. The sample contained particles from three size ranges, with the average sizes being 5.1 µm, 14.3 µm and 31.5 µm. The image shows that the particles have separation at the outlet, with largest 31.5 µm sized particles going to the inner wall outlet, and small 5.1 µm and medium 14.3 µm sized particles going to the outer wall outlet. This is evidence of the device's sorting capabilities.

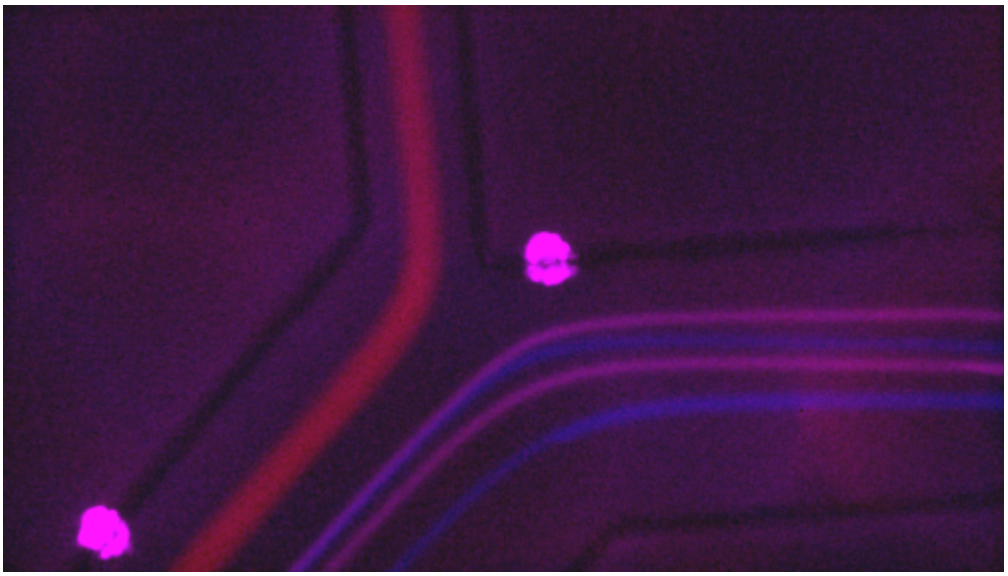

Figure 15. Composite image of PDMS chip outlet region with fluorescent particles. Separation of the particles is visible with the larger and wider red stripes corresponding to the largest 31.5 µm particles, and the thinner blue and purple striper corresponding to medium 14.3 µm and smallest 5.1 µm sized particles. Particle velocity is 170 mm/s and the figure consists of three images overlayed. Two purple-coloured objects are particles stuck to the channel walls.

Figure 15 is a composite of three images from the outlet region. The light source is a UV lamp, and a red filter is used. The images are combined using ImageJ software, and its *merge channels* feature. The colours on the lines are assigned based on the fluorescent emission colour of the particles. Red for the largest size, purple for the medium, and blue for the smallest. The combined flow rate of sheath and sample pumps used for that measurement is 850 µl/min. Using equation 1, the average velocity the particle experience in the channel is thus 170 mm/s.

Simulations were made with the geometry used in the PDMS chips. COMSOL software was used to determine which flow rates would have a 100% accumulation of the largest sized particles into the inner wall outlet. The separation is heavily affected by the flow rates, as much as 10-20% increase or decrease from optimal was observed in both simulations and measurements to lose all separation of the particles. The simulation model is shown in Figure 16. Inlet region is omitted for ease in modelling and computation.

With simulations, velocities from 100 mm/s to 260 mm/s were tested. Based on the simulations, a trend seems to be that higher flow rates have higher count of the largest sized particles in the inner wall outlet. With velocities over 220 mm/s, all the largest particles migrated to the inner wall outlet. From Figure 17, it can be seen that the amount of large particles increased in the simulations when the flow rates were higher. This trend holds to a certain threshold, until all the particles will migrate to the inner wall outlet.

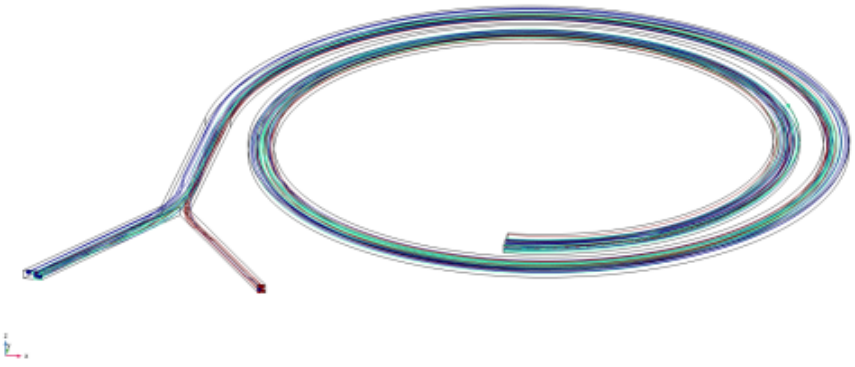

Figure 16. Simulation using spiral device geometry and three size ranged particles to study the effect of flow rate on the sorting efficiency of the device. Simulations done on COMSOL.

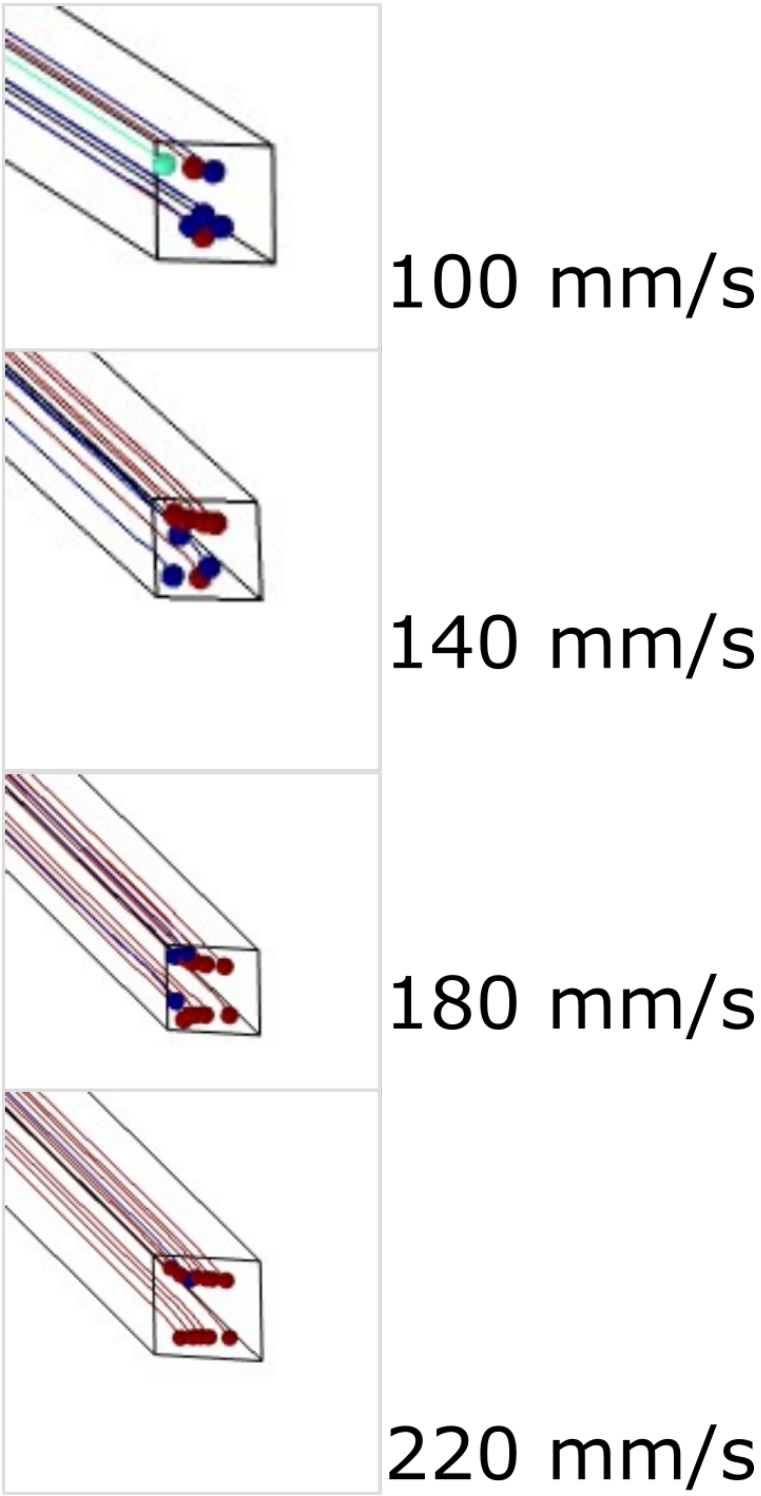

Figure 17. The effect of flow rates on the amount of large particles in the inner wall outlet. Higher flow rate means more 31.5 µm particles, in a certain velocity range.

A 100% accumulation of large particles was sought to obtain in experimental results as well. Mirroring the results from simulations, and from a similar device made by Warkiani et al. [1], velocities ranging from 170 mm/s to 180 mm/s were tested. The accumulation of the largest sized particles between the two outlets is shown in Figure 18. The velocity with best accumulation is 170 mm/s, with a 94% accumulation. The measurements do not seem to reflect the trend from the simulations, but they also did not have as large of a range.

With the 170 mm/s velocity, particle distribution at the outlets is shown in Figure 19. Most of the 31.5 µm particles were counted at the inner wall outlet, as desired. Inversely, most of 5.1 µm and 14.3 µm particles were counted at the outer wall outlet. From the data, the depletion rate in the device for 14.3 µm particles was 99.97%.

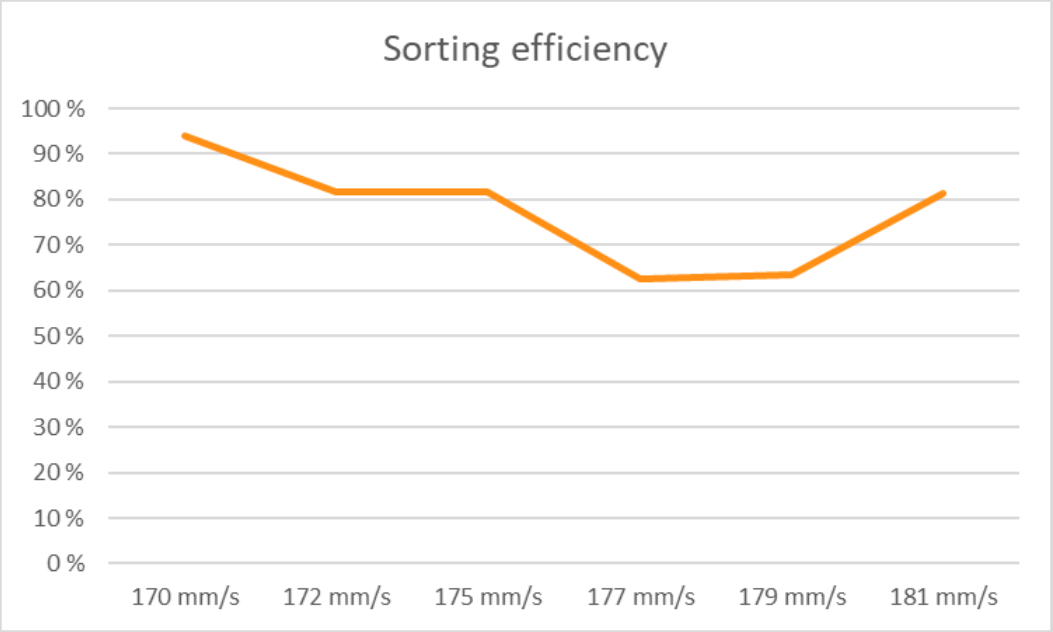

Figure 18. A graph showing the sorting efficiency of the device. Largest particles gathered at the inner wall outlet versus outer wall outlet with respect to increasing flow velocities. The trend seems to be inferior efficiency with increased flow rate.

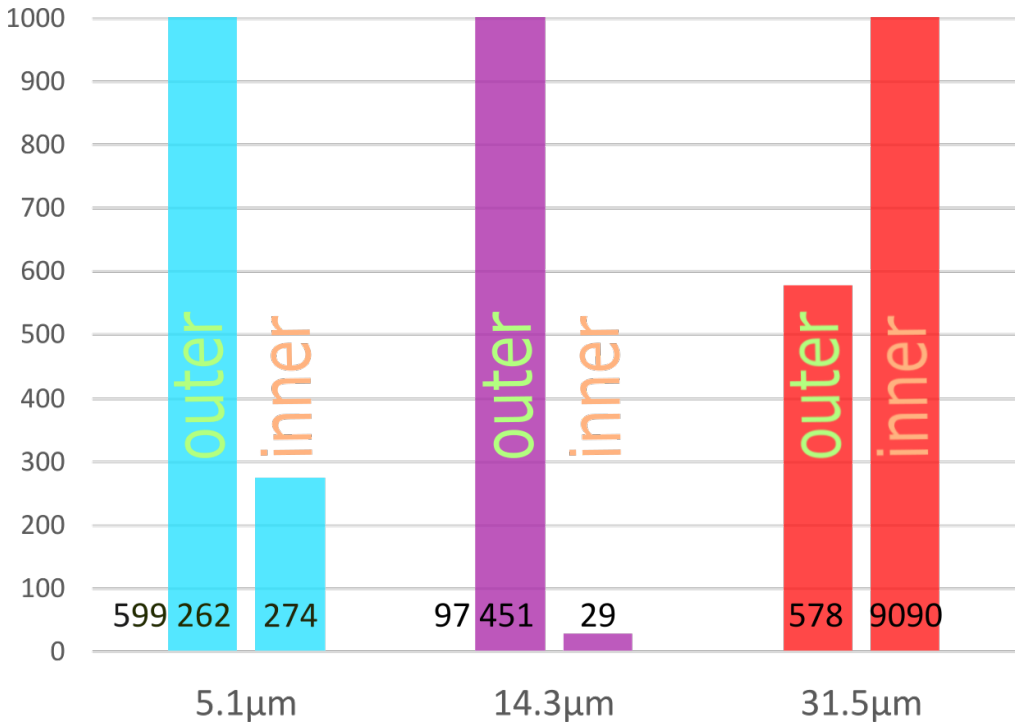

Figure 19. Particle distribution at 170 mm/s particle velocity. The bar chart has been capped at 1000 to show differences between outlets, the actual numbers are written on the columns. Columns are from smallest particle size to largest from left to right. Smallest particles are most common in outer wall outlet, as well as medium sized ones. The largest particles have migrated to the inner wall outlet.

These numbers are comparable to the device made earlier by Warkiani et al [1]. It is a similarly sized spiral device used in the same flow rate range. Their experiment was with tumour cells in blood, which do differ from particles in a buffer solution. However, the device made in this research could be used for the same purpose. They reported $\geq 85\%$ recovery of the largest cells, which are in the size range of the largest 31.5 µm particles. Then, it is a smaller sorting efficiency. However, they reported a slightly larger white blood cell depletion of 99.99%.

Devices with multiple loops have also been researched previously. A 5-loop spiral microchannel device by Kuntaegowdanahalli et al. exhibited a 90% separation efficiency with 10 µm, 15 µm, and 20 µm polystyrene particles [23]. Their channel dimensions are comparable to the one made here, 500 µm in width and 130 µm in height. Also, their archimedean device was capable of 80% efficiency with neuroblastoma and glioma cells. This puts the device at slightly lower percentages than this study's device. A smaller device also containing five loops was fabricated by Bhagat et al.[25]. It was capable of complete separation of 7.3 µm and 1.9 µm particles.

The separation efficiency of spiral microfluidic devices have also been tested stacked together. Kim et al. made a sheathless cascaded spiral device which achieved 86.76% recovery of cancer cells and 97.91% depletion rate of leukocytes [26]. Some research have also been done with other than rectangular channels. For example, Wu et al. made a spiral device with a trapezoidal cross-section [24]. It is capable of high efficiency (>80%), separating leukocytes from blood. Additionally, a multiple loop spiral device made by Shen et al. had micro-obstacles embedded on the channel walls [27]. That device achieved a 98.7% sorting efficiency for 15.5µm sized particles and >95% for CTCs. The device made in this study then has similar or better performance when compared to similar device designed previously in research.

5 Discussion

The results obtained with the device designed in the study are promising. With a wider range of flow rates, a 100% accumulation of the largest sized particles could be done. Ultimately, there is a trade-off between the highest possible accumulation of largest particles and highest possible depletion of other sizes. Especially, if the device is used with cells, as they have more size range overlap. As the device is intended to be used with rare tumour cells, it would be ideal to collect them all.

There are two notable facets in which the results could be improved upon. The first is channel clogging. Fibres and air bubbles are the largest impediments found in the measurements for the PDMS chips. Fibres can get stuck to the channel walls crosswise and block the liquid flow, completely or from either outlet. Their presence can also disrupt the lateral migration of particles. Air bubbles are a similar problem. They also affect the hydrodynamics of the system and are harder to prevent. Increased pressure and increased flow rates were used to remove these obstructions, and no data was collected during such times. The improve the situation, the set-up could be modified to include valves or gates, for example, to prevent air from entering the channels.

The other facet is image analysis. Currently, some particles are excluded from the count due to their proximity to the channel wall. There isn't enough contrast between the wall and the particles. Neglecting the wall's presence would be desirable. Similarly, the processing is ineffective if the particles are very clustered. It happens particularly, if the suspension solution is not optimal, the sample concentration is too high, or if there is no stirring or other such movement on the sample syringe. All these are addressed in the measurements, but could be extended to image analysis as well.

On top of that, while the number of particles counted within this study is large, the number of measurements per flow rate was only two to four. Statistically, while one measurement usually contained a couple of image stacks, it is a small amount of data. More could be done to minimise error. For instance, the variation of sorting efficiency to flow rate was not as linear as expected. With only a few measurements

per flowrate, any variation due to air bubbles or equivalent will have a large impact on the sorting efficiency reported. The trend observed for sorting efficiency, shown in Figure 18, could be suffering from this as it does not have an expected or consistent shape. Furthermore, all the measurements were done with a single chip. There can be some defects or wear that can impact the function. For more valid results, multiple chips should be tested for consistency.

6 Conclusions

In this study, a spiral microfluidic sorting device was developed. It can separate particles based on their size at high throughput and efficiency. First, it was demonstrated that the designed geometry and dimensions of the device made it suitable for its purpose. Then, its performance was measured to be as good as or superior to other devices of similar nature previously reported. The sorting efficiency was 94% for the 31.5 µm sized particles. The sorting device is simple to fabricate, and multiple quantities can be made in little time by using the fabrication recipe. The materials for the device are relatively low cost making it desirable for many applications. The device relies on passive forces, and with optimised operation conditions, using it is very straightforward. Some enhancements, such as additional components, could be added to minimise contaminants and obtrusions in the device, such as air bubbles.

Since the device performed well with particle sorting, it is expected that cell separation could be achieved as well. Other research groups have had success in that area with very similar devices, capable of sorting both particles and cells with good efficiency. Converting the set-up to work with cells could be as simple as slightly tuning the parameters. The flow rates at which sorting efficiency is optimal for cells is expected to be different than for particles, due to difference is density, deformation, and interactions. When the device is optimised for cells, it could be used to separate circulating tumour cells from other blood components, as the tumour cells tend to be larger in size.

In the futue, the aim is to optimise the device to collect all the tumour cells from blood so they can be analysed further. The tumour cells are quite rare in blood samples, which is why a sorting device is useful for analysis and why it is important to achieve as large of a sorting efficiency as possible. The device made in this study would act as a pre-concentrator, enriching the amount of tumour cells present in the sample. The device is intended to be combined with another to remove any other cells that were not depleted by the pre-concentrator. That could be achieved with more active sorting, i.e., the separation would be based on other properties of the cells. By combining the pre-concentrator and the active sorting, potentially all of

the tumour cells present in the blood could be acquired without other blood cells contaminating the sample. Once the device or devices are operational, they could be utilised in cancer treatment. Particularly, in treatment screening by testing the treatment options on cultured tumour cells obtained from the sorting.

References

[1] M. E. Warkiani et al. “Ultra-fast, label-free isolation of circulating tumor cells from blood using spiral microfluidics”. In: *Nature protocols* 11 (1 2015), pp. 134–148.

[2] B. R. Mutlu et al. “Non-equilibrium Inertial Separation Array for High-throughput, Large-volume Blood Fractionation”. In: *Scientific Reports* 7 (1 2017).

[3] J. F. Edd et al. “Microfluidic concentration and separation of circulating tumor cell clusters from large blood volumes”. In: *Lab Chip* 20 (3 2020), pp. 558–567.

[4] P. K. Panigrahi. *Transport Phenomena in Microfluidic Systems*. John Wiley & Sons, 2016.

[5] J. Berthier and P. Silberzan. *Microfluidics for Biotechnology*. 2nd ed. Artech House, 2010.

[6] P. Tabeling. *Introduction to Microfluidics*. 2nd ed. Oxford University Press, 2006.

[7] F. Vollrath and D. Knight. “Structure and function of the silk production pathway in the Spider Nephila edulis”. In: *International Journal of Biological Macromolecules* 24.2 (1999), pp. 243–249.

[8] A. Eichmann and D. M. Greif. “Brain vessels squeezed to death”. In: *Nature* 508 (7494 2014), pp. 50–51.

[9] Q. Guo et al. “Deformability based Cell Sorting using Microfluidic Ratchets Enabling Phenotypic Separation of Leukocytes Directly from Whole Blood”. In: *Scientific Reports* 7 (1 2017).

[10] N. Futai et al. “Handheld recirculation system and customized media for microfluidic cell culture”. In: *Lab Chip* 6 (1 2006), pp. 149–154.

[11] F. Dingfelder et al. “Rapid Microfluidic Double-Jump Mixing Device for Single-Molecule Spectroscopy”. In: *Journal of the American Chemical Society* 139.17 (2017), pp. 6062–6065.

[12] C.-J. Kim. “Microfluidics using the surface tension force in microscale”. In: *Microfluidic Devices and Systems III*. Ed. by C. H. Mastrangelo and H. Becker. Vol. 4177. International Society for Optics and Photonics. SPIE, 2000, pp. 18–24.

[13] S.-J. J. Lee and N. Sundararajan. *Microfabrication for Microfluidics*. Artech House, 2010.

[14] *Flow Rate and Its Relation to Velocity*. [Online; accessed 2021-07-13]. July 11, 2021. URL: https://phys.libretexts.org/@go/page/1571.

[15] G. I. Taylor. “The criterion for turbulence in curved pipes”. In: *Proceedings of the Royal Society of London. Series A, Containing Papers of a Mathematical and Physical Character* 124.794 (1929), pp. 243–249.

[16] B. Liptak. *Flow Measurement*. Taylor & Francis, 1993.

[17] NuclearPower. *Friction Factor for Laminar Flow*. https://www.nuclear-power.net/nuclear-engineering/fluid-dynamics/major-head-loss-friction-loss/friction-factor-for-laminar-flow/. (Visited on 07/13/2021).

[18] N. Nivedita, P. M. Ligrani, and I. Papautsky. “Evolution of secondary Dean vortices in spiral microchannel for cell separations”. In: Engineering. 2013.

[19] J. Berthier. “From Microfluidics for Biotechnology to Biomicrofluidics”. In: Technical Proceedings of the NSTI Nanotechnology Conference and Expo. 2013.

[20] Y. Gou et al. “Progress of Inertial Microfluidics in Principle and Application”. In: *Sensors* 18.6 (2018).

[21] N. Liu et al. “Spiral Inertial Microfluidics for Cell Separation and Biomedical Applications”. In: *Applications of Microfluidic Systems in Biology and Medicine*. Ed. by M. Tokeshi. Springer Singapore, 2019, pp. 99–150.

[22] M. Asghari et al. “Tape’n roll inertial microfluidics”. In: *Sensors and Actuators A: Physical* 299 (2019), p. 111630.

[23] S. S. Kuntaegowdanahalli et al. “Inertial microfluidics for continuous particle separation in spiral microchannels”. In: *Lab Chip* 9 (20 2009), pp. 2973–2980.

[24] L. Wu et al. “Separation of Leukocytes from Blood Using Spiral Channel with Trapezoid Cross-Section”. In: *Analytical Chemistry* 84.21 (2012), pp. 9324–9331.

[25] A. A. S. Bhagat, S. S. Kuntaegowdanahalli, and I. Papautsky. “Continuous particle separation in spiral microchannels using dean flows and differential migration”. In: *Lab Chip* 8 (11 2008), pp. 1906–1914.

[26] T. H. Kim et al. “Cascaded spiral microfluidic device for deterministic and high purity continuous separation of circulating tumor cells”. In: *Biomicrofluidics* 8.6 (2014), p. 064117.

[27] S. Shen et al. “Spiral microchannel with ordered micro-obstacles for continuous and highly-efficient particle separation”. In: *Lab Chip* 17 (21 2017), pp. 3578–3591.